HYDROTHERMALLY SYNTHESIZED h-MoO_3 AND α-MoO_3 NANOCRYSTALS: NEW FINDINGS ON CRYSTAL STRUCTURE DEPENDENT CHARGE TRANSPORT

A. CHITHAMBARARAJ[a], N. RAJESWARI YOGAMALAR[b] AND A. CHANDRA BOSE[a]

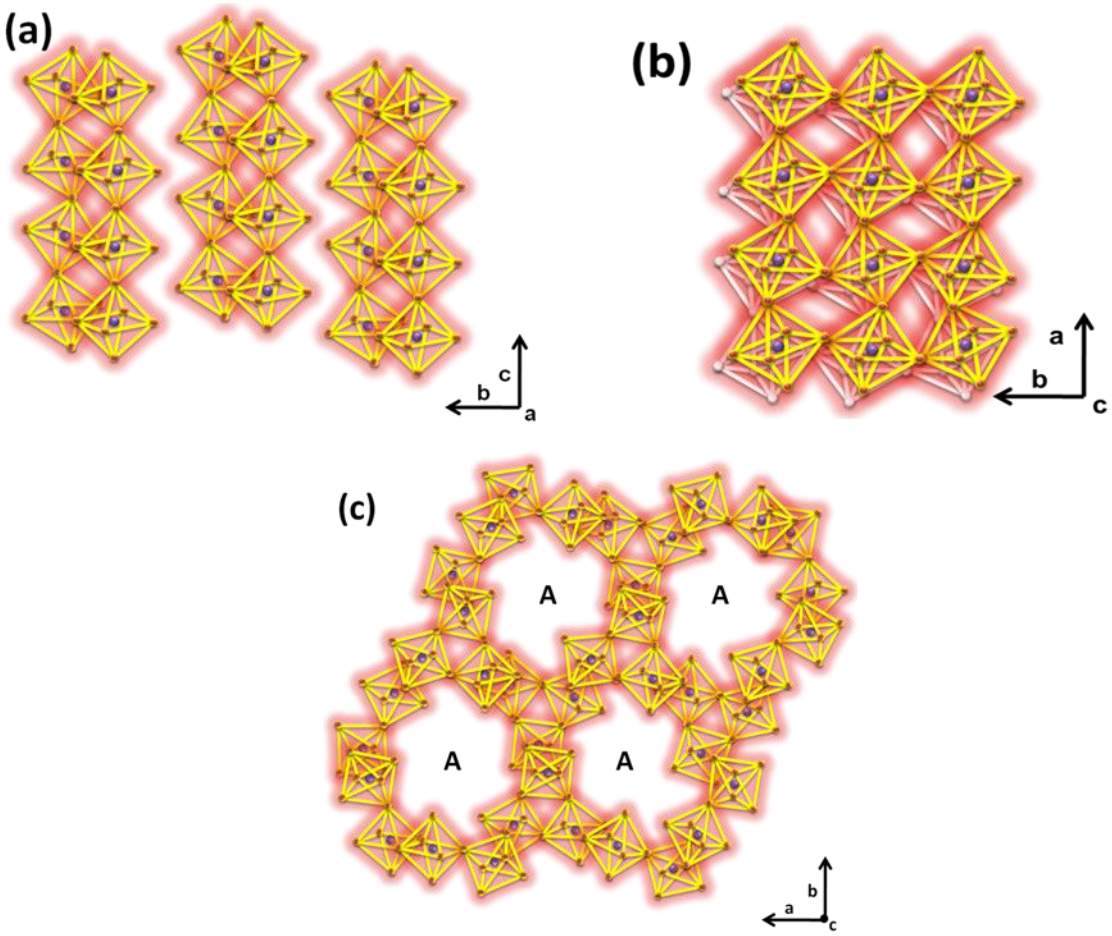

(ESI†) S1. Different crystal structures of MoO_3: (a) α-MoO_3, (b) β-MoO_3, and (c) h-MoO_3.

HYDROTHERMALLY SYNTHESIZED h-MoO_3 AND α-MoO_3 NANOCRYSTALS: NEW FINDINGS ON CRYSTAL STRUCTURE DEPENDENT CHARGE TRANSPORT

A. CHITHAMBARARAJ[a], N. RAJESWARI YOGAMALAR[b] AND A. CHANDRA BOSE[a]

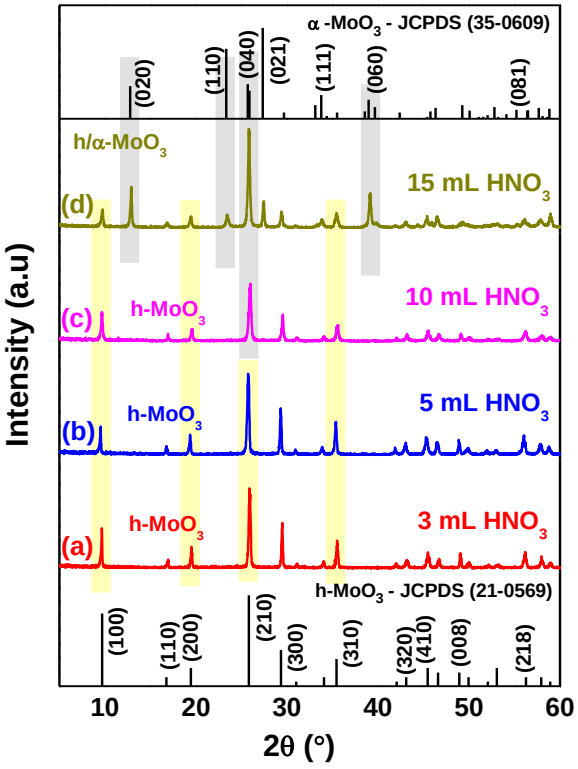

(ESI†) S2. XRD patterns of as-synthesized samples prepared with (a) 3 mL; (b) 5 mL; (c) 10 mL and (d) 15 mL HNO_3

HYDROTHERMALLY SYNTHESIZED h-MoO_3 AND α-MoO_3 NANOCRYSTALS: NEW FINDINGS ON CRYSTAL STRUCTURE DEPENDENT CHARGE TRANSPORT

A. CHITHAMBARARAJ[a], N. RAJESWARI YOGAMALAR[b] AND A. CHANDRA BOSE[a]

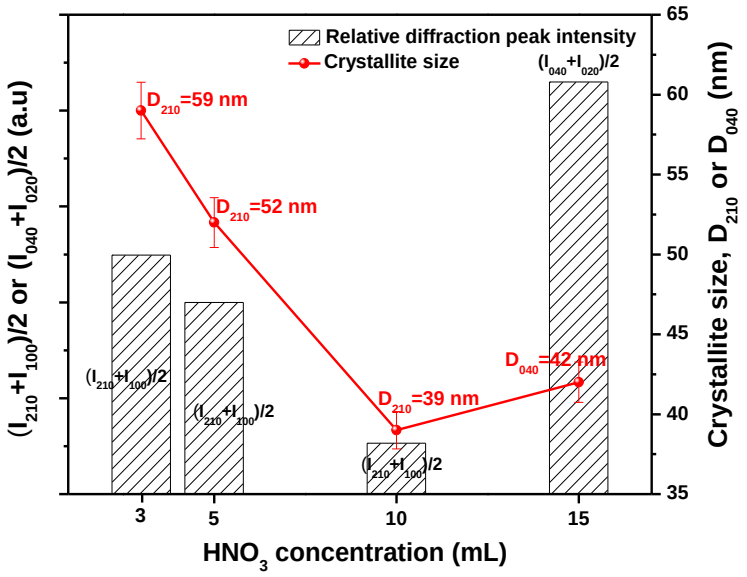

(ESI†) S3. Relative diffraction peak intensity and the variation of the crystallite size as a function of amount of HNO_3

HYDROTHERMALLY SYNTHESIZED h-MoO_3 AND α-MoO_3 NANOCRYSTALS: NEW FINDINGS ON CRYSTAL STRUCTURE DEPENDENT CHARGE TRANSPORT

A. CHITHAMBARARAJ[a], N. RAJESWARI YOGAMALAR[b] AND A. CHANDRA BOSE[a]

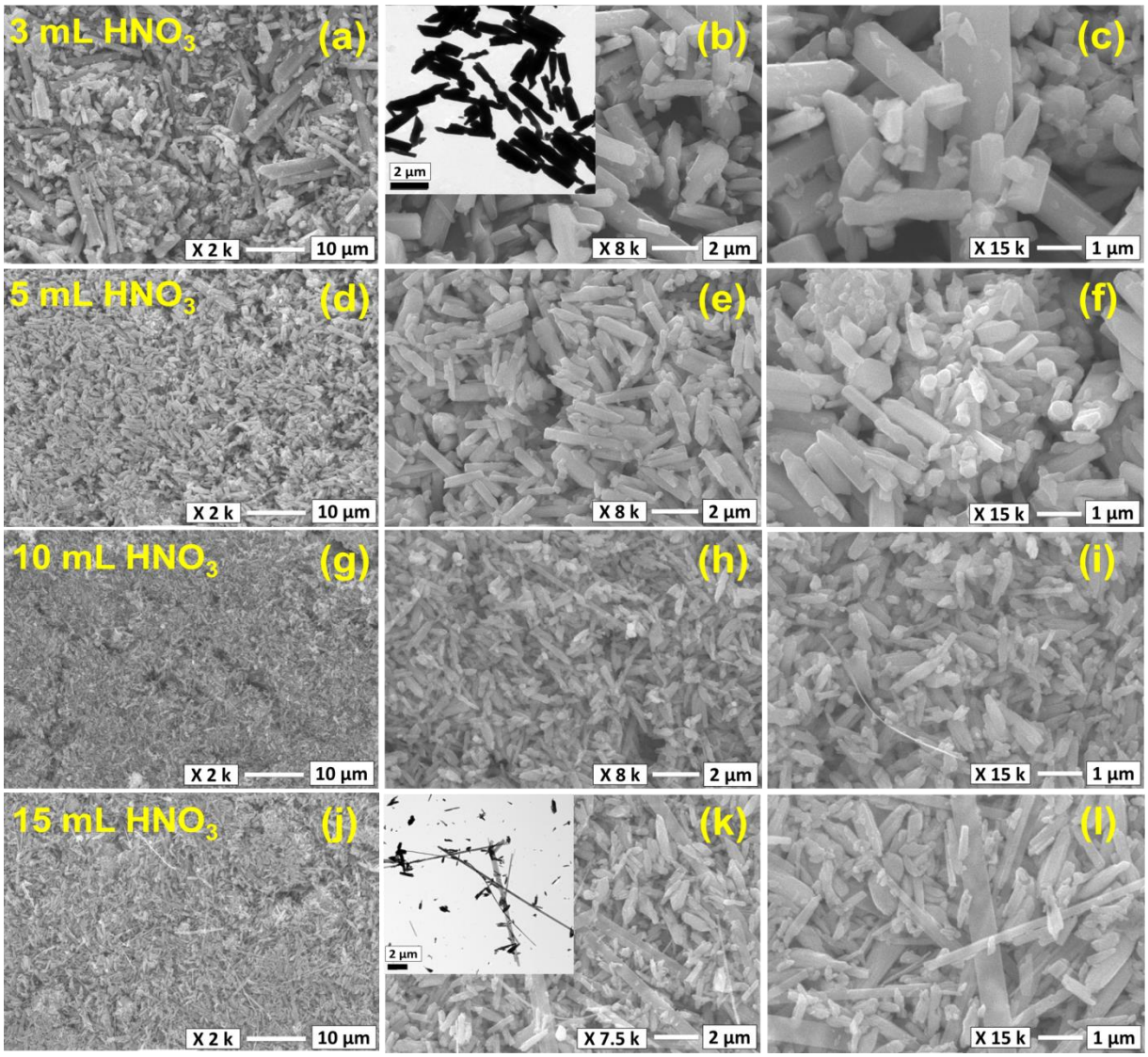

(ESI†) S4. SEM images of the as-synthesized MoO_3 samples prepared for varying amount of HNO_3 (a-c) 3 mL, (d-f) 5 mL, (g-i) 10 mL and (j-l) 15 mL HNO_3; The insets in Fig. S4-b and Fig. S4-k represents the TEM images of as-synthesized samples for 3 mL and 15 mL HNO_3, respectively

HYDROTHERMALLY SYNTHESIZED h-MoO_3 AND α-MoO_3 NANOCRYSTALS: NEW FINDINGS ON CRYSTAL STRUCTURE DEPENDENT CHARGE TRANSPORT

A. CHITHAMBARARAJ[a], N. RAJESWARI YOGAMALAR[b] AND A. CHANDRA BOSE[a]

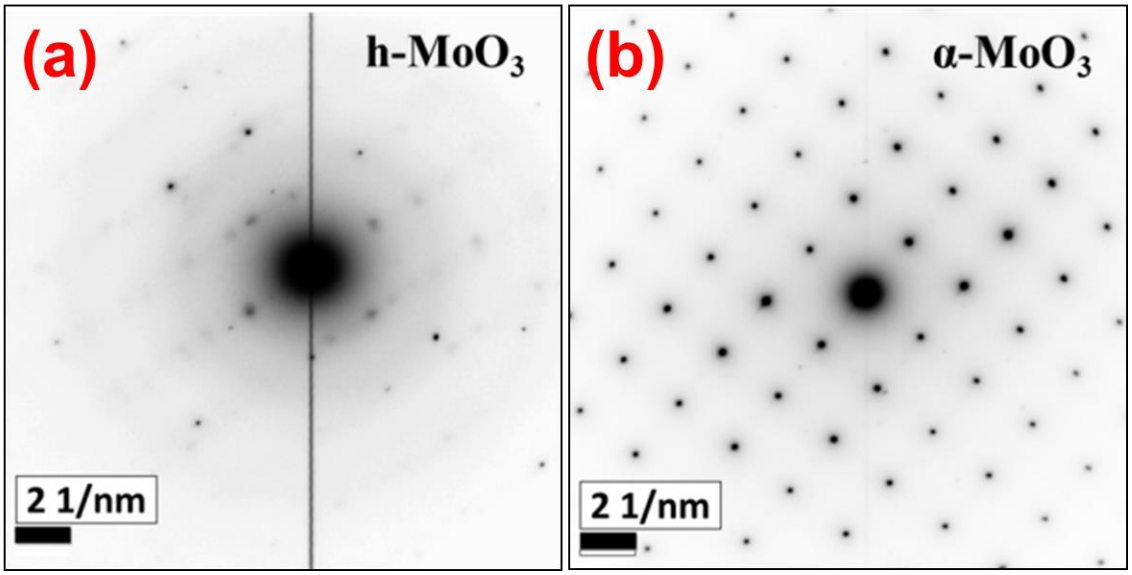

(ESI†) S5 The SAED patterns of (a) h-MoO_3 and (b) α-MoO_3

HYDROTHERMALLY SYNTHESIZED h-MoO_3 AND α-MoO_3 NANOCRYSTALS: NEW FINDINGS ON CRYSTAL STRUCTURE DEPENDENT CHARGE TRANSPORT

A. CHITHAMBARARAJ[a], N. RAJESWARI YOGAMALAR[b] AND A. CHANDRA BOSE[a]

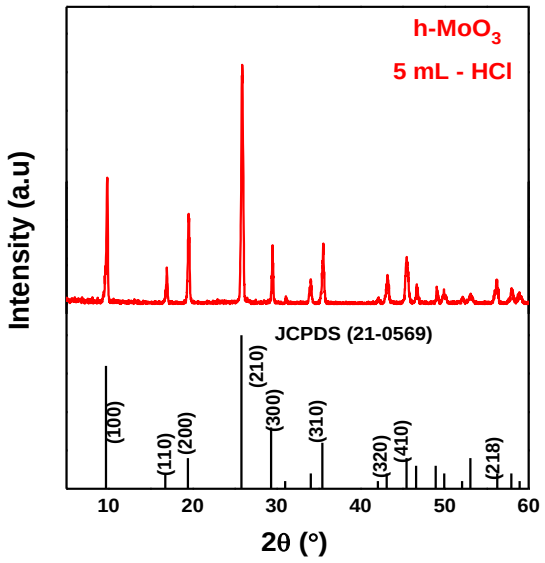

(ESI†) S6 XRD pattern of the as-synthesized sample prepared using 5 mL concentration of HCl

HYDROTHERMALLY SYNTHESIZED h-MoO_3 AND α-MoO_3 NANOCRYSTALS: NEW FINDINGS ON CRYSTAL STRUCTURE DEPENDENT CHARGE TRANSPORT

A. CHITHAMBARARAJ[a], N. RAJESWARI YOGAMALAR[b] AND A. CHANDRA BOSE[a]

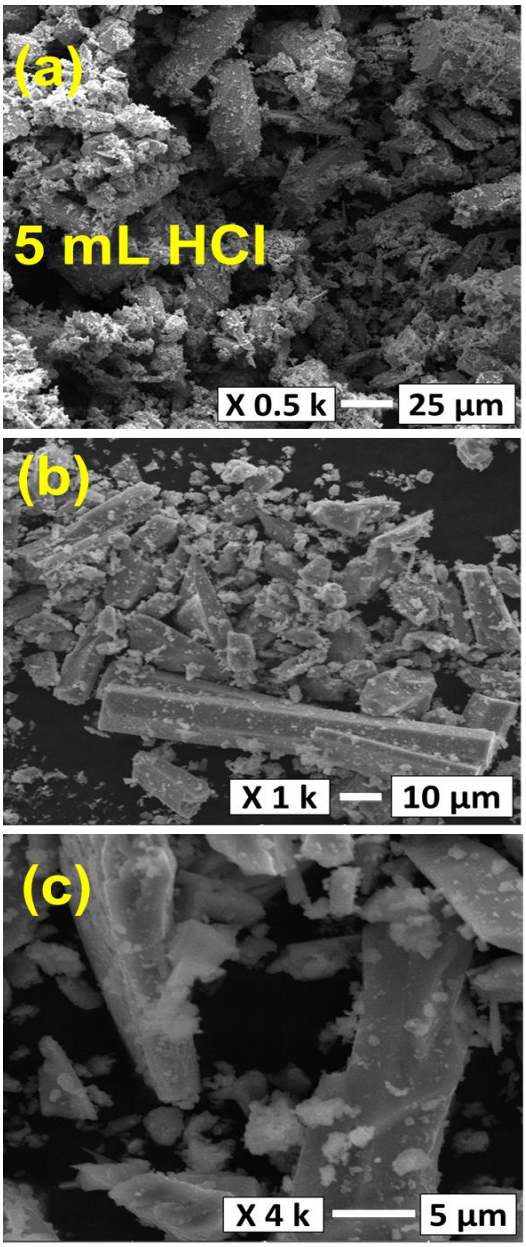

(ESI†) S7 (a and b) Low and (c) high magnified SEM images of the as-synthesized h-MoO_3 synthesized 5 mL concentration of HCl

HYDROTHERMALLY SYNTHESIZED h-MoO_3 AND α-MoO_3 NANOCRYSTALS: NEW FINDINGS ON CRYSTAL STRUCTURE DEPENDENT CHARGE TRANSPORT

A. CHITHAMBARARAJ[a], N. RAJESWARI YOGAMALAR[b] AND A. CHANDRA BOSE[a]

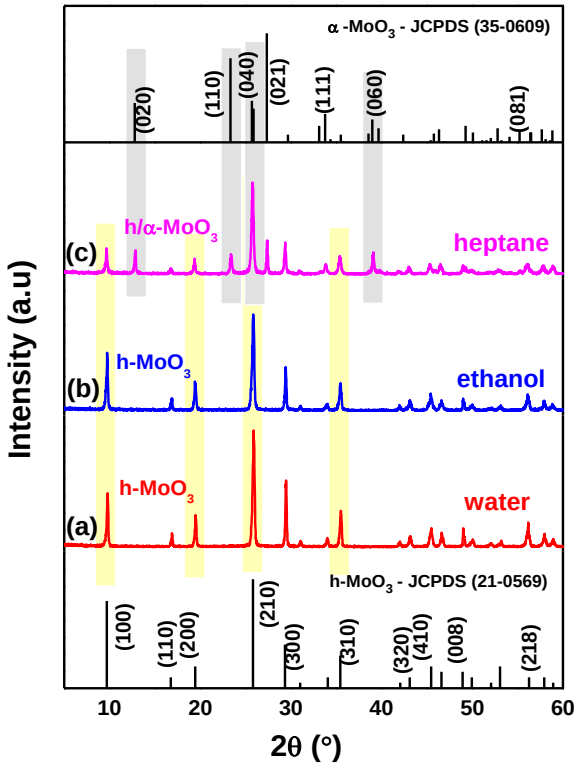

(ESI†) S8. XRD pattern of as-synthesized samples prepared using (a) water, (b) ethanol and (c) heptane as hydrothermal reactant medium

HYDROTHERMALLY SYNTHESIZED h-MoO_3 AND α-MoO_3 NANOCRYSTALS: NEW FINDINGS ON CRYSTAL STRUCTURE DEPENDENT CHARGE TRANSPORT

A. CHITHAMBARARAJ[a], N. RAJESWARI YOGAMALAR[b] AND A. CHANDRA BOSE[a]

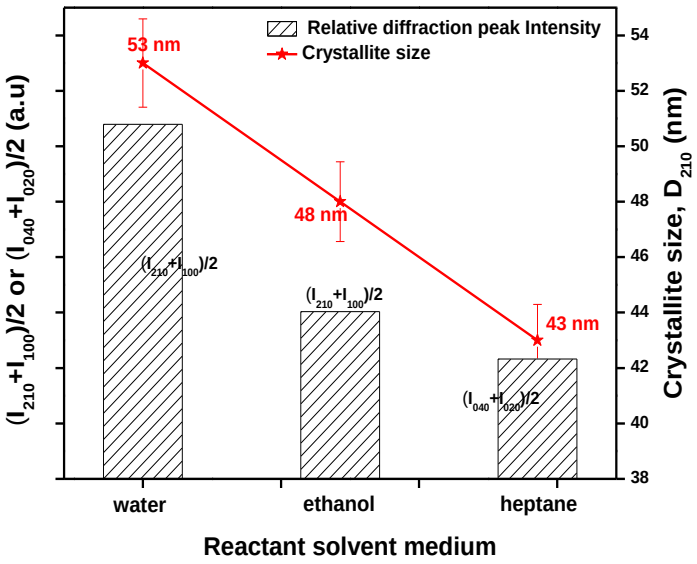

(ESI†) S9 Relative diffraction peak intensity and the variation of crystallite size as a function of reactant solvent medium

HYDROTHERMALLY SYNTHESIZED h-MoO_3 AND α-MoO_3 NANOCRYSTALS: NEW FINDINGS ON CRYSTAL STRUCTURE DEPENDENT CHARGE TRANSPORT

A. CHITHAMBARARAJ[a], N. RAJESWARI YOGAMALAR[b] AND A. CHANDRA BOSE[a]

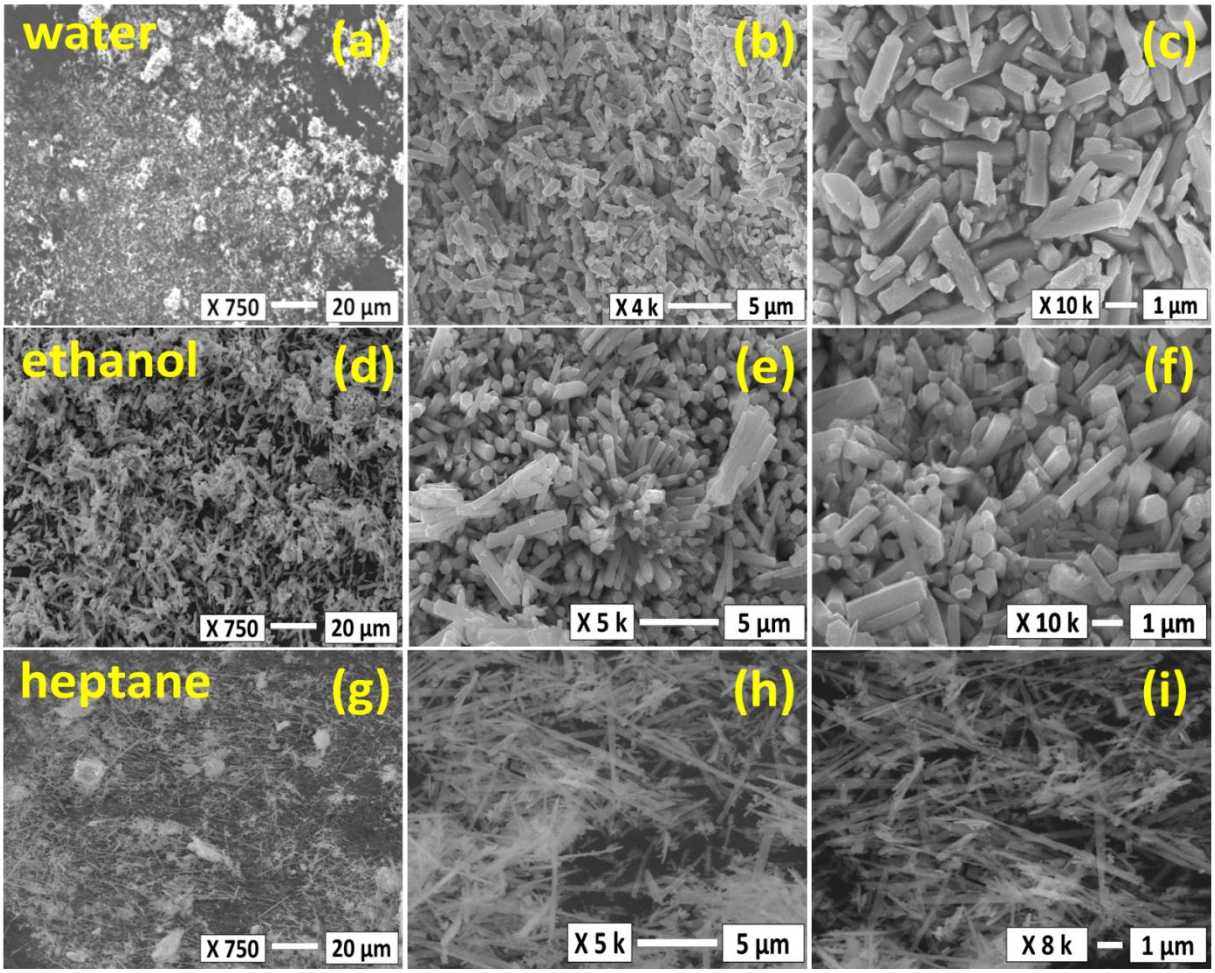

(ESI†) S10. Low and high magnification SEM images of as-synthesized MoO_3 samples prepared using (a-c) water; (d-f) ethanol and (g-i) heptane as hydrothermal reactant medium

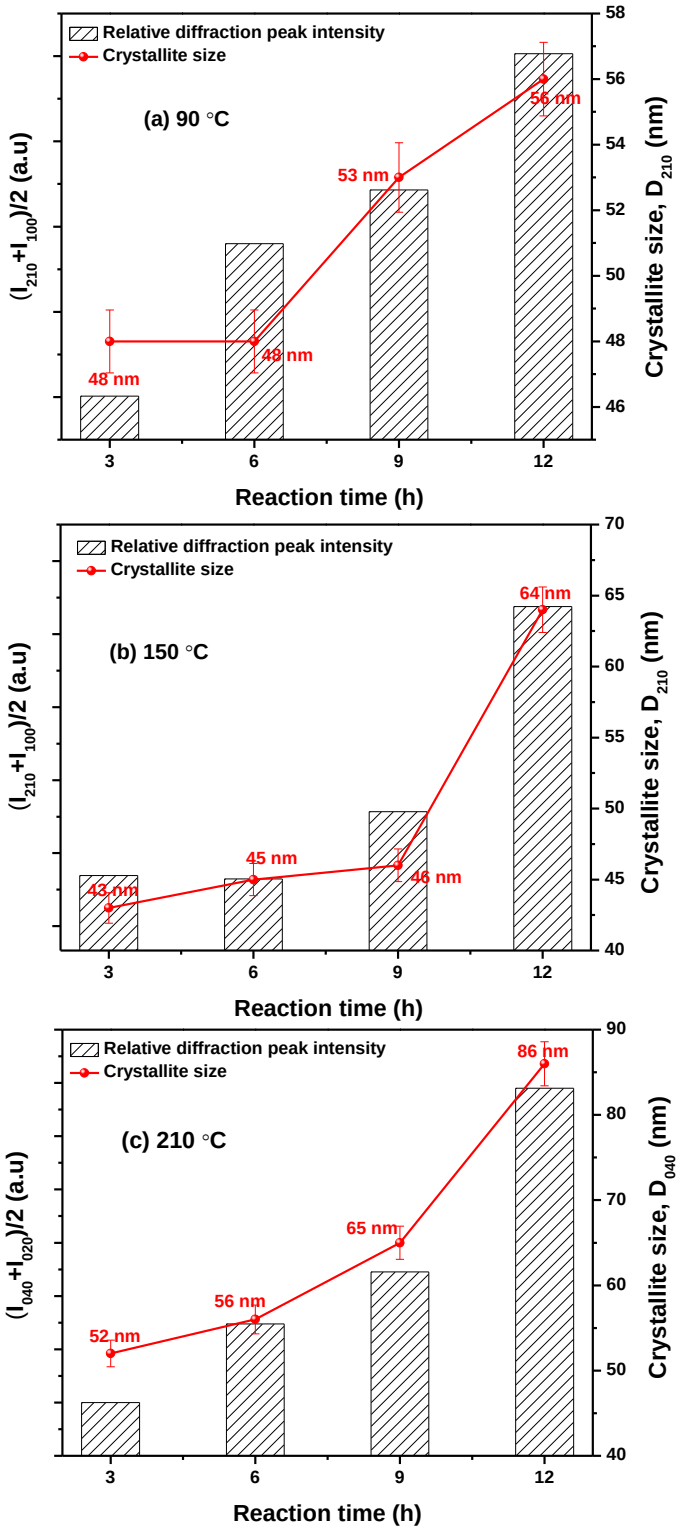

(ESI†) S11. Relative diffraction peak intensity and the variation of the crystallite size for the samples synthesized at 90 °C; (b) 150 °C and (c) 210 °C for different times.

HYDROTHERMALLY SYNTHESIZED h-MoO_3 AND α-MoO_3 NANOCRYSTALS: NEW FINDINGS ON CRYSTAL STRUCTURE DEPENDENT CHARGE TRANSPORT

A. CHITHAMBARARAJ[a], N. RAJESWARI YOGAMALAR[b] AND A. CHANDRA BOSE[a]

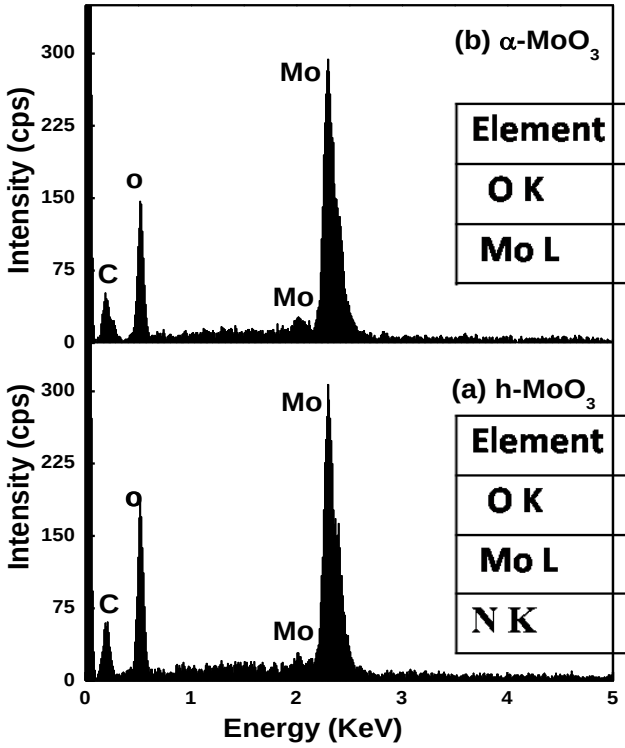

Element	Weight %	Atomic%
O K	28.26	70.25
Mo L	71.74	29.75

Element	Weight %	Atomic%
O K	31.53	66.62
Mo L	63.97	22.53
N K	4.50	10.85

(ESI†) S12. EDS spectra of **(a)** h-MoO_3 and **(b)** α-MoO_3 samples synthesized at 90 °C and 210 °C for 9 h, respectively

HYDROTHERMALLY SYNTHESIZED h-MoO_3 AND α-MoO_3 NANOCRYSTALS: NEW FINDINGS ON CRYSTAL STRUCTURE DEPENDENT CHARGE TRANSPORT

A. CHITHAMBARARAJ[a], N. RAJESWARI YOGAMALAR[b] AND A. CHANDRA BOSE[a]

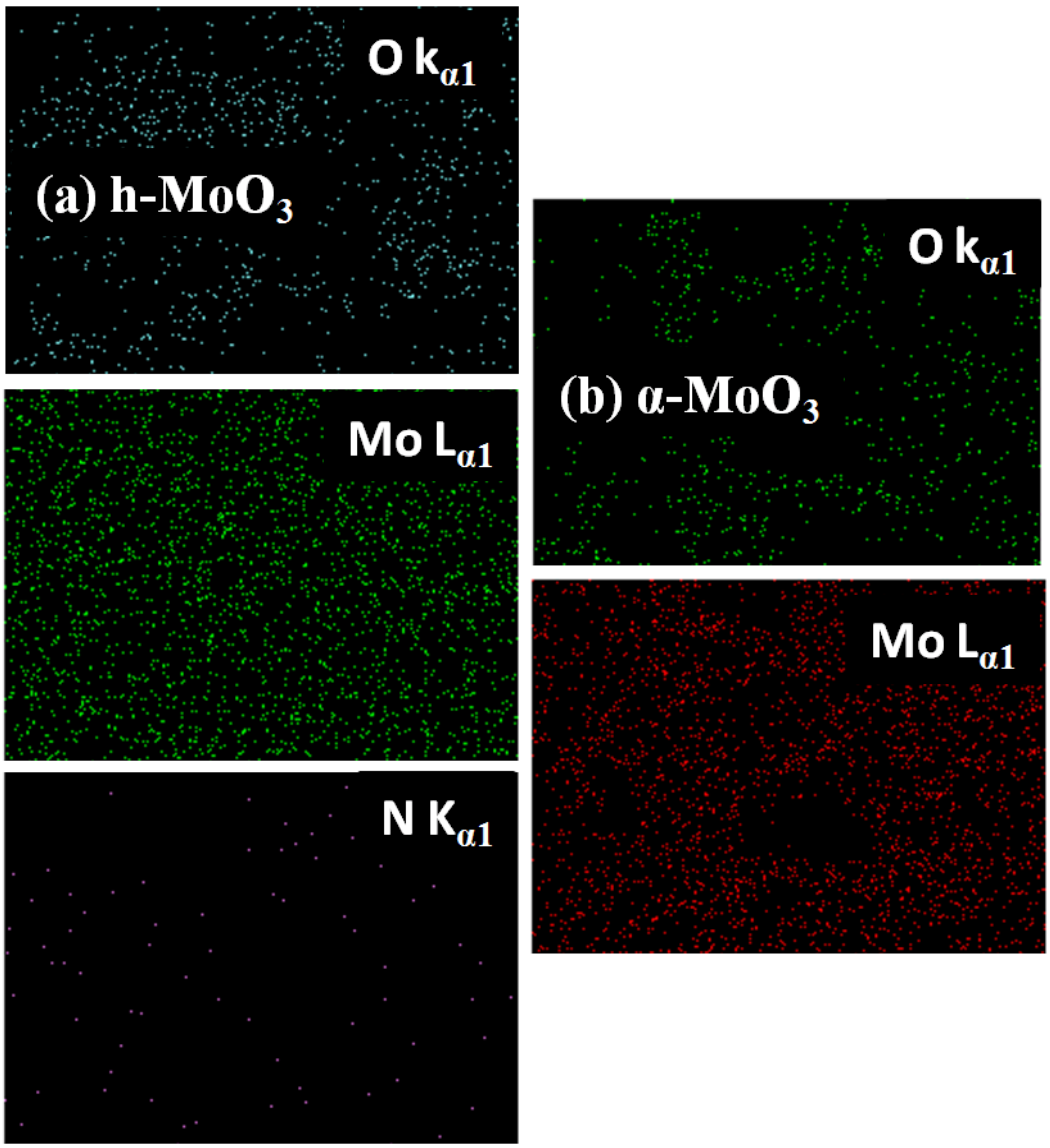

(ESI†) S13. Elemental map of **(a)** h-MoO_3 and **(b)** α-MoO_3 samples synthesized at 90 °C and 210 °C for 9 h, respectively

HYDROTHERMALLY SYNTHESIZED h-MoO_3 AND α-MoO_3 NANOCRYSTALS: NEW FINDINGS ON CRYSTAL STRUCTURE DEPENDENT CHARGE TRANSPORT

A. CHITHAMBARARAJ[a], N. RAJESWARI YOGAMALAR[b] AND A. CHANDRA BOSE[a]

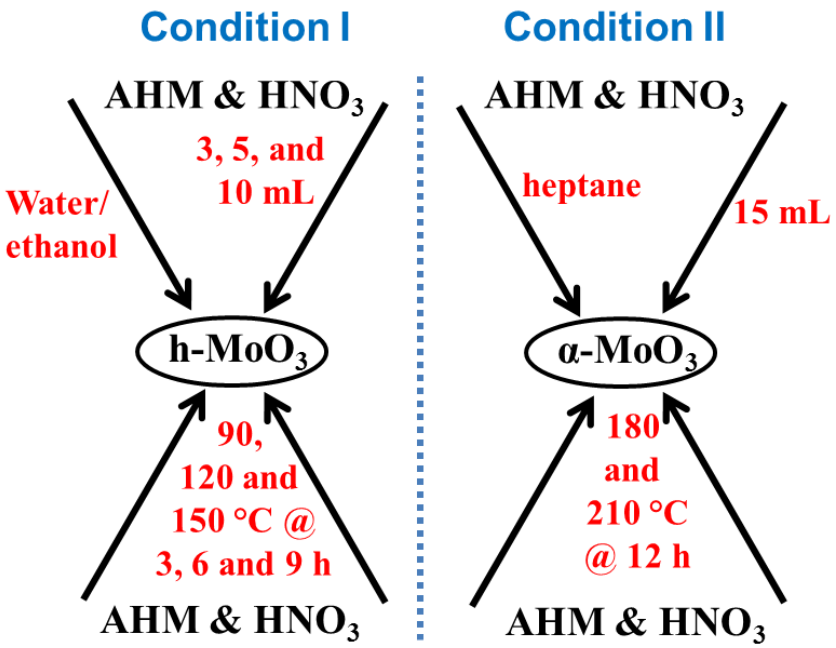

(ESI†) S14. Role of hydrothermal reaction conditions towards the selective phase synthesis of MoO_3 nanocrystals

HYDROTHERMALLY SYNTHESIZED h-MoO_3 AND α-MoO_3 NANOCRYSTALS: NEW FINDINGS ON CRYSTAL STRUCTURE DEPENDENT CHARGE TRANSPORT

A. CHITHAMBARARAJ[a], N. RAJESWARI YOGAMALAR[b] AND A. CHANDRA BOSE[a]

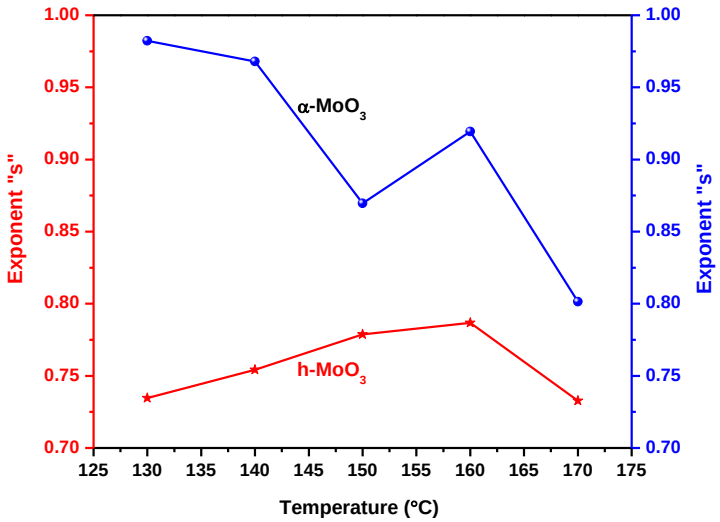

(ESI†) S15. Variation of "s" with respect to temperature for h-MoO_3 and α-MoO_3.